



Relationship between the loading rate of inorganic mercury to aquatic ecosystems and dissolved gaseous mercury production and evasion

Alexandre J. Poulain^{a,*,1}, Diane M. Orihel^{b,c,1}, Marc Amyot^a, Michael J. Paterson^c, Holger Hintelmann^d, George R. Southworth^e

^a *Département de Sciences Biologiques, Université de Montréal, C.P. 6128, Succursale Centre-Ville, Pavillon Marie-Victorin, Montréal, QC, Canada H3C 3J7*

^b *Clayton H. Riddell Faculty of Environment, Earth, and Resources, University of Manitoba, Winnipeg, MB, Canada R3T 2N2*

^c *Freshwater Institute, Fisheries and Oceans Canada, 501 University Crescent, Winnipeg, MB, Canada R3T 2N6*

^d *Department of Chemistry, Trent University, 1600 West Bank Drive, Peterborough, ON, Canada K9J 7B8*

^e *Environmental Sciences Division, Oak Ridge National Laboratory, Building 1505, P.O. Box 2008 MS6036, Oak Ridge, TN 37831-6036, United States*

Received 17 January 2006; received in revised form 29 May 2006; accepted 30 May 2006

Abstract

The purpose of our study was to test the hypothesis that dissolved gaseous mercury (DGM) production and evasion is directly proportional to the loading rate of inorganic mercury [Hg(II)] to aquatic ecosystems. We simulated different rates of atmospheric mercury deposition in 10-m diameter mesocosms in a boreal lake by adding multiple additions of Hg(II) enriched with a stable mercury isotope (²⁰²Hg). We measured DGM concentrations in surface waters and estimated evasion rates using the thin-film gas exchange model and mass transfer coefficients derived from sulfur hexafluoride (SF₆) additions. The additions of Hg(II) stimulated DGM production, indicating that newly added Hg(II) was highly reactive. Concentrations of DGM derived from the experimental Hg(II) additions (“spike DGM”) were directly proportional to the rate of Hg(II) loading to the mesocosms. Spike DGM concentrations averaged 0.15, 0.48 and 0.94 ng l⁻¹ in mesocosms loaded at 7.1, 14.2, and 35.5 μg Hg m⁻² yr⁻¹, respectively. The evasion rates of spike DGM from these mesocosms averaged 4.2, 17.2, and 22.3 ng m⁻² h⁻¹, respectively. The percentage of Hg(II) added to the mesocosms that was lost to the atmosphere was substantial (33–59% over 8 weeks) and was unrelated to the rate of Hg(II) loading. We conclude that changes in atmospheric mercury deposition to aquatic ecosystems will not change the relative proportion of mercury recycled to the atmosphere.

© 2006 Elsevier Ltd. All rights reserved.

Keywords: Dissolved gaseous mercury; Evasion; Atmospheric deposition; Stable isotope; Sulfur hexafluoride; METAALICUS

1. Introduction

The production of dissolved gaseous mercury (DGM) and its subsequent evasion to the atmosphere is a critical

pathway in the biogeochemical cycle of mercury in aquatic ecosystems. DGM refers to volatile mercury species present in water and is essentially composed of elemental mercury in freshwaters (Vandal et al., 1991; Tseng et al., 2004). DGM is produced by the reduction of divalent mercury, Hg(II), by abiotic or biotic processes (e.g. Alberts et al., 1974; Amyot et al., 1994; Mason et al., 1995; Siciliano et al., 2002). The production and evasion of DGM reduces the pool of Hg(II) in aquatic systems available

* Corresponding author. Tel.: +1 514 343 6111x3188; fax: +1 514 343 2293.

E-mail address: alexandre.poulain@umontreal.ca (A.J. Poulain).

¹ These authors contributed equally to this paper.

for conversion to methylmercury (“reactive Hg(II) substrate hypothesis”; Fitzgerald et al., 1991), which is well-known to be a neurotoxin that bioaccumulates in food webs.

For many aquatic ecosystems, the primary source of Hg(II) is atmospheric deposition of anthropogenic mercury emissions (Jackson, 1997; Fitzgerald et al., 1998). Little is known, however, about the relationship between the rate of atmospheric Hg(II) deposition and the production and evasion of DGM. Previous studies suggest that DGM production may be limited by the supply of Hg(II) (e.g. Amyot et al., 1997, 2000), but it has not been established whether DGM production in natural ecosystems is directly proportional to the rate of Hg(II) deposition. This question is critical to understanding the potential effectiveness of current proposals to reduce anthropogenic emissions of mercury to the atmosphere. If changes in atmospheric mercury deposition result in disproportional changes in DGM production and evasion, this could affect the pool of Hg(II) available for conversion to methylmercury, possibly hampering the effectiveness of emission reductions.

The purpose of our study was to test the hypothesis that DGM production and evasion is directly proportional to the rate of Hg(II) loading to aquatic ecosystems. In the MESOSIM experiment (MESOCOSM SIMulations of atmospheric mercury deposition to aquatic ecosystems), we simulated different rates of atmospheric Hg(II) deposition in 10-m diameter mesocosms in a boreal lake. The MESOSIM experiment is a part of the METAALICUS initiative (Mercury Experiment To Assess Atmospheric Loading In Canada and the United States) to examine the effects of changes in atmospheric Hg(II) deposition on mercury biogeochemical cycling and methylmercury bioaccumulation in aquatic food webs. The MESOSIM experiment builds upon an earlier pilot study conducted by Amyot et al. (2004), in which Hg(II) was added to mesocosms to simulate an atmospheric deposition rate of $30 \mu\text{g m}^{-2}$. Because Hg(II) was only added at one loading rate, this earlier study could not address the relationship between the rate of Hg(II) loading and DGM production and evasion.

To simulate atmospheric Hg(II) deposition in the mesocosms, we added a solution highly enriched in a stable mercury isotope (^{202}Hg). The addition of isotope-enriched mercury allowed us to monitor concentrations of DGM in surface waters derived from the experimental Hg(II) additions, and relate these concentrations to Hg(II) loading rates. We estimated mercury evasion rates based on the thin-film gas exchange model, using sulfur hexafluoride (SF_6) as a tracer for gas exchange. Our objectives in this paper were: (i) to examine the relationship between Hg(II) loading rates and concentrations of DGM derived from the experimental Hg(II) additions; and (ii) to estimate the proportion of experimentally added mercury lost to the atmosphere and determine if this loss was affected by the rate of Hg(II) loading.

2. Methods

2.1. Experimental design

In June 2002, 11 mesocosms were installed in the littoral zone of Lake 240 at the Experimental Lakes Area (ELA; Ontario, Canada, $49^{\circ}40'N$ $93^{\circ}44'W$). Mesocosms were 10-m diameter, polyvinyl tubes enclosing a 2-m water column and open to the air and sediments. Inorganic mercury (90.9% ^{202}Hg ; Trace Sciences International) was added to the mesocosms to simulate different Hg(II) wet deposition rates. Mercury was added to the mesocosms in eight equal additions. Additions were performed once a week between 26 June and 14 August 2002. For each addition, the isotope-enriched solution (HgCl_2 in 5% nitric acid) was added to 500 mL lake water, injected below the water surface at dusk (as recommended by Amyot et al., 2004), and mixed into the water column with an electric motor. Three mesocosms, loaded at 2 \times , 5 \times , and 12 \times annual wet deposition at the ELA ($7.1 \mu\text{g Hg m}^{-2} \text{yr}^{-1}$; St. Louis et al., 2001), are the focus of this paper. Mesocosms 2 \times , 5 \times , and 12 \times received 134, 336, and 807 $\mu\text{g Hg}$ during each weekly addition, respectively. Water volumes and chemistry of the mesocosms are provided in Table 1. Although mercury was added as an inorganic dissolved compound, we recognize that mercury can be associated with other species (organic) and phases (aerosols) dissolved in water droplets present in the atmosphere. It is likely that both the organic and/or particulate fraction will affect the reactivity of mercury upon its entrance into surface waters and therefore affect its evasion. In this study, however, we could not assess the fate of mercury in the particulate and organic fractions from the atmosphere.

2.2. Sample collection and analysis

Surface water samples for determination of DGM concentrations were collected before and after the 2nd, 4th, 6th, and 8th Hg(II) addition. Water was sampled three times around each Hg(II) addition: on the day of the addition (day 0), one day after the addition (day 1), and three days after the addition (day 3). On two occasions, samples were collected one day late due to inclement weather. On every sampling date, duplicate samples were collected from each mesocosm between 10:00 and 14:00. Samples were collected by manually immersing a 1-l Teflon bottle below the surface and capping it underwater leaving no headspace. Teflon bottles were acid-washed prior to use, stored in clean plastic bags, and handled with non-powdered gloves. During transport to the laboratory, samples were kept in the dark and at 4°C .

Within 3 h of collection, samples were processed at the ELA laboratory. Five hundred milliliters of each water sample was poured into an amber gas-washing bottle and sparged for 20 min with ultra-high-purity argon. Volatile mercury species were captured on a gold trap attached to the outlet of the gas-washing bottle. Gold traps were sealed

Table 1
Characteristics of the mesocosms and the surrounding lake (mean and SD, $n = 5$)

Characteristic	Units	Meso 2×	Meso 5×	Meso 12×	Lake 240
Volume	m ³	132	147	132	–
Alkalinity	μeq l ⁻¹	138 (8)	141 (13)	152 (13)	132 (2)
pH		7.1	7.1	7.3	7.1
Conductivity	μS cm ⁻¹	24 (2)	24 (2)	25 (2)	24 (1)
Suspended carbon	μg l ⁻¹	994 (577)	982 (357)	802 (82)	704 (92)
Dissolved organic carbon	μg l ⁻¹	8297 (678)	8335 (513)	7485 (557)	7752 (360)
Dissolved inorganic carbon	μg l ⁻¹	1578 (101)	1557 (145)	1698 (198)	1494 (57)
Suspended nitrogen	μg l ⁻¹	89 (32)	103 (20)	80 (8)	69 (16)
Total dissolved nitrogen	μg l ⁻¹	359 (53)	350 (40)	313 (27)	323 (17)
Nitrate	μg l ⁻¹	3 (2)	4 (3)	3 (1)	2 (1)
Nitrite	μg l ⁻¹	<1	<1	<1	<1
Ammonia	μg l ⁻¹	17 (5)	21 (11)	34 (32)	26 (25)
Suspended phosphorus	μg l ⁻¹	5 (1)	6 (1)	5 (0)	4 (1)
Total dissolved phosphorus	μg l ⁻¹	3 (1)	3 (1)	3 (1)	2 (1)
Chlorophyll <i>a</i>	μg l ⁻¹	2.15 (0.67)	2.66 (1.20)	2.27 (0.52)	2.52 (1.15)
Ambient Hg _T in unfiltered water	ng l ⁻¹	2.05 (0.89)	2.65 (1.30)	1.78 (0.70)	1.62 (0.24)

with Teflon plugs and stored in an airtight container filled with nitrogen. At Trent University (Peterborough, Ontario), gold traps were analyzed by inductively coupled plasma mass spectrometry (ICP/MS; Thermo-Finnigan Element2) to determine individual mercury isotope concentrations (Hintelmann and Ogrinc, 2003). The typical procedural detection limit for this method was 2 pg Hg l⁻¹. For quality control, a subset of samples was also analyzed at the ELA within 4 h of collection using the double amalgamation technique described in Poulain et al. (2004). No significant difference in total DGM concentrations was observed between duplicate samples analyzed at the ELA and Trent University (paired *t*-test, $t = 1.75$, $p > 0.05$, $n = 40$).

Comparing the mercury isotope composition of samples to natural mercury isotope ratios allowed us to determine the amount of mercury in a sample from the experimental Hg(II) additions (Hintelmann and Ogrinc, 2003). We refer to the experimentally added mercury as “spike mercury”, and the mercury naturally present as “ambient mercury”. Spike mercury is calculated by dividing the amount of ²⁰²Hg in a sample in excess of its natural abundance by the proportion of ²⁰²Hg in the mercury preparation added to the mesocosms (i.e. 0.91). In this paper, we abbreviate dissolved gaseous spike mercury as “spike DGM”, and dissolved gaseous ambient mercury as “ambient DGM”.

2.3. Estimation of mercury evasion

2.3.1. Thin-film model

We estimated mercury evasion, f (ng m⁻² h⁻¹), based on the thin-film gas exchange model (Liss and Slater, 1974; Vandal et al., 1991):

$$f = k_{\text{Hg}} \left(C_w - \frac{C_a}{H} \right) \quad (1)$$

where k_{Hg} the mass transfer coefficient of elemental mercury (cm h⁻¹), C_w is the concentration of DGM, either ambient or spike, in surface water (ng m⁻³), C_a is the con-

centration of elemental mercury in the atmosphere (ng m⁻³), and H is Henry's law constant (dimensionless unit). The concentration of mercury in air was measured directly over each of the intensive mesocosms on 20 July, 4 August, and 19 August 2002. A known volume of air was drawn through a gold trap for 1 h, and the mass of mercury on the gold trap was analyzed by ICP/MS. The average (\pm SD) concentration of mercury in air was 2.0 ± 1.2 ng m⁻³ ($n = 9$). We assumed that C_a was 2 ng m⁻³ in all flux calculations. We used the same value of C_a regardless of whether we were calculating the flux of spike DGM or ambient DGM. H was corrected for temperature, T (°C), using the formula developed by Sanemasa (1975):

$$H = 0.0074T + 0.1551 \quad (2)$$

2.3.2. Mass transfer coefficient

We added SF₆, a chemically and biologically non-reactive gas, to the mesocosms as a tracer for gas exchange (e.g. Wanninkhof et al., 1985). On 1, 15, 19 July, and 12 August, SF₆ gas was injected into a polyethylene bottle containing lake water, shaken for 2 min, and released underwater in the mesocosms. Surface water samples for determination of SF₆ concentration were collected, in triplicate, between 3–8 July, 17–20 July, 31 July–3 August, and 14–19 August (corresponding to DGM monitoring periods). Samples were collected by puncturing a 50 mL evacuated serum bottle (containing 5 mL ultra-high-purity nitrogen) held under the water surface, and were analyzed by gas chromatography (Varian 3800) at the Freshwater Institute (Winnipeg, Manitoba) following the methods described in Matthews et al. (2003).

The mass transfer coefficient of SF₆, k_{SF_6} (cm h⁻¹), was calculated from Wanninkhof et al. (1985):

$$k_{\text{SF}_6} = h \cdot \frac{d \ln C_{\text{SF}_6}}{dt} \quad (3)$$

where h is the mean depth of the mesocosm (cm), C_{SF_6} is the concentration of SF₆ in surface water, and t is time (h).

The mass transfer coefficient of elemental mercury, k_{Hg} (cm h^{-1}), was determined from k_{SF_6} using a formula adapted from Jähne et al. (1987):

$$k_{\text{Hg}} = k_{\text{SF}_6} \left(\frac{Sc_{\text{SF}_6}}{Sc_{\text{Hg}}} \right)^{\frac{2}{3}} \quad (4)$$

where Sc_{SF_6} and Sc_{Hg} are the Schmidt numbers for SF_6 and elemental mercury (dimensionless units), respectively. Following Crusius and Wanninkhof (2003), the exponent in Eq. (4) was assumed to be $2/3$ because wind speeds did not exceed 3 m s^{-1} during this experiment.

As described in Poissant et al. (2000), but originally defined by Boucher and Alves (1959), Sc_{Hg} can be directly derived from its definition (i.e. kinematic viscosity of water (v)/diffusion coefficient of the gas (D)), with

$$v = 0.017e^{-0.025T} \quad (5)$$

$$D = 6 \times 10^{-7}T + 1 \times 10^{-5} \quad (6)$$

Sc_{SF_6} was calculated using the empirical formula developed by Wanninkhof (1992):

$$Sc_{\text{SF}_6} = 3255.3 - 217.13T + 6.8370T^2 - 0.086070T^3 \quad (7)$$

2.3.3. Cumulative loss of mercury

We estimated the cumulative loss of mercury to the atmosphere over a period of time by summing the mass of mercury evaded each day of the period. First, since we did not carry out diel cycles, we assumed that DGM concentrations measured between 10:00 and 14:00 were representative of a 24-h period. Differences in DGM concentrations between day and night at the ELA are less extreme than in other locations. For example, in a previous mesocosm experiment conducted at the ELA, mid-day concentrations of DGM were only 1.2 times higher than midnight values (Amyot et al., 2004). Because we did not adjust for decreases in DGM concentrations during the night, our estimates of cumulative loss should be considered as upper values. As our objective in this study was to examine relative differences in evasion among mesocosms, this bias does not affect our conclusions. Second, because DGM concentrations were not measured after every Hg(II) addition, we estimated these DGM concentrations using linear interpolations between comparable days. For example, we interpolated days 0, 1, and 3 of each non-monitored Hg(II) addition based on days 0, 1, and 3, respectively, of the previous and following monitored Hg(II) addition. We interpolated all remaining days based on the two nearest data points. Third, we assumed that k_{SF_6} during periods when SF_6 was not monitored was equal to the mean k_{SF_6} of the four periods when SF_6 was monitored.

2.4. Data analysis

We tested the hypothesis that DGM production was proportional to the loading rate of Hg(II) to the mesocosms. Because we examined DGM production in only

three mesocosms, a regression approach was not appropriate for this data set. Rather, we tested this hypothesis by comparing observed DGM concentrations to those expected if this hypothesis was true. This was possible since the mass transfer coefficients we calculated (see Section 3.2.) were not greatly different between the three mesocosms, and evasion consequently had the same effect on net concentrations of DGM measured in the water column. We generated one expected concentration for each observed concentration by assuming strict proportionality among mesocosms. To achieve this, we first summed the spike DGM concentrations in Mesocosm 2 \times , 5 \times , and 12 \times on each sampling day. Then, we multiplied each sum: by $2/(2+5+12)$ to obtain the expected values for Mesocosm 2 \times , by $5/(2+5+12)$ to obtain the expected values for Mesocosm 5 \times ; and by $12/(2+5+12)$ to obtain the expected values for Mesocosm 12 \times . For each mesocosm, we used a Wilcoxon Matched Pairs test (Statistica 6.1) to determine whether the observed values and the values expected assuming a proportional relationship were significantly different. Because data for each test was collected within one mesocosm, this test was conservative with respect to our conclusions.

3. Results and discussion

3.1. Dissolved gaseous mercury concentrations

Spike DGM concentrations ranged from 0.04–0.27 ng l^{-1} in Mesocosm 2 \times , 0.09–1.09 ng l^{-1} in Mesocosm 5 \times , and 0.26–1.47 ng l^{-1} in Mesocosm 12 \times (Fig. 1; circles). In comparison, concentrations of ambient DGM were similar among mesocosms and averaged $0.12 \pm 0.025 \text{ ng l}^{-1}$. Concentrations of spike DGM in Mesocosm 2 \times were within the range of DGM values reported for natural lakes with no point source of mercury pollution (e.g. Fitzgerald et al., 1994; Mason et al., 1995; O'Driscoll et al., 2003), but the upper range of spike DGM concentrations in Mesocosms 5 \times and 12 \times have only been reported previously in mercury-contaminated sites (Ganguli et al., 2000; Feng et al., 2004). The average (\pm SD) ratio of spike DGM over ambient DGM was 1.2 ± 0.6 in Mesocosm 2 \times , 3.7 ± 2.1 in Mesocosm 5 \times , and 7.6 ± 3.7 in Mesocosm 12 \times .

The addition of inorganic mercury [Hg(II)] to the mesocosms readily stimulated the production of DGM. Spike DGM concentrations measured one day after each Hg(II) addition were substantially higher (up to 225%) than the previous day. These high levels of spike DGM were short-lived, as concentrations measured three days after each Hg(II) addition were considerably lower. Accordingly, concentrations of spike DGM in the mesocosms followed a saw-tooth pattern over time (Fig. 1; circles). We also observed that spike DGM tended to accumulate over time (Fig. 1; circles), suggesting there were two pools of spike Hg(II) available for reduction; one from the most recent Hg(II) addition, and one from previous Hg(II) additions. In contrast to changes over time in spike DGM,

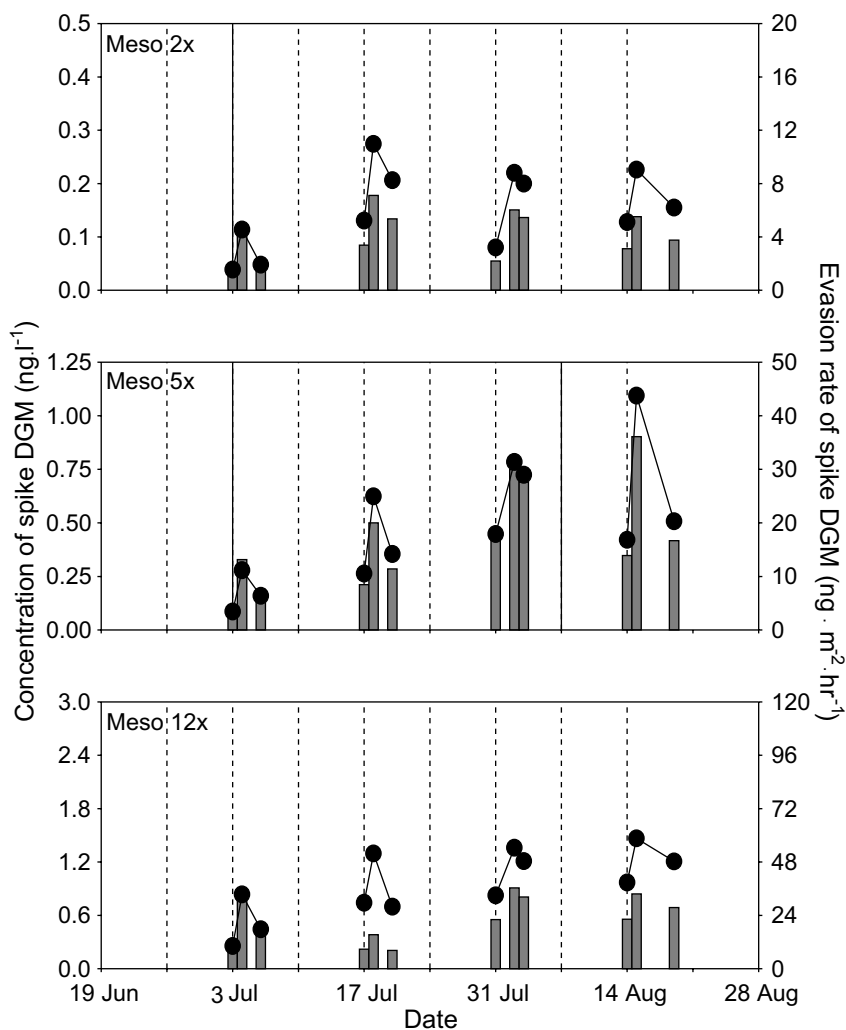


Fig. 1. Temporal changes in the surface water concentration (circles; left axis) and evasion rate (columns; right axis) of spike DGM in each mesocosm. Vertical lines indicate dates of Hg(II) additions. Y-axes are proportional to Hg(II) loading rates.

ambient DGM concentrations were relatively constant during the experiment ($0.07\text{--}0.17\text{ ng l}^{-1}$).

The increase in spike DGM observed one day after Hg(II) additions suggests that newly added Hg was highly reactive and that DGM production in the mesocosms was substrate-limited in the water column. The decrease in spike DGM in the mesocosms between one and three days after Hg(II) additions was likely caused by several processes: (i) evasion of spike DGM to the atmosphere; (ii) decline in DGM production rates as the pool of spike Hg(II) in the mesocosms decreased in quantity and/or quality; and (iii) oxidation of spike DGM back to Hg(II). The peaks in spike DGM concentrations in the mesocosms following Hg(II) additions resemble changes in DGM concentrations in surface waters of natural lakes following rain events (Vandal et al., 1995; Amyot et al., 2000; Lindberg et al., 2000).

Spike DGM concentrations were strongly related to the rate of inorganic Hg(II) loading to the mesocosms. Spike DGM concentrations consistently increased with Hg(II)

loading rate on all sampling dates (Fig. 2; bars). In most cases, observed concentrations of spike DGM were similar to those expected if DGM production were directly proportional to Hg(II) loading rates (Fig. 2; diamonds). We observed no significant differences between observed and expected concentrations of spike DGM for any of the mesocosms (Wilcoxon Matched Pairs Test; Mesocosm 2x: $T = 20$, $p = 0.23$; Mesocosm 5x: $T = 16$, $p = 0.07$; Mesocosm 12x: $T = 26$, $p = 0.31$), supporting the hypothesis that DGM production is directly proportional to the rate of Hg(II) loading to aquatic ecosystems. All p -values were not significant regardless of whether or not a Bonferroni correction was applied.

This study is the first to demonstrate a directly proportional relationship between the rate of Hg(II) loading and concentrations of DGM in surface waters. Because concentrations of total mercury in water, derived from the experimental additions, were also directly proportional to Hg(II) loading rates in the mesocosms (Orihel, 2005), we believe DGM production was directly proportional to the avail-

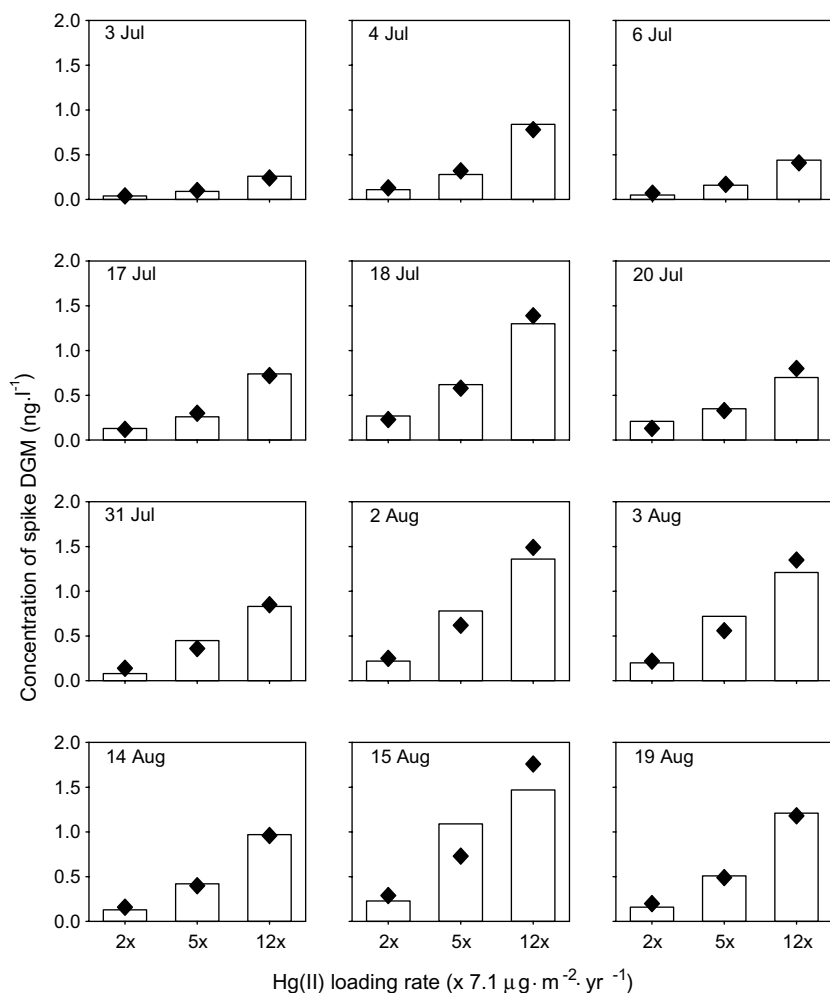


Fig. 2. Relationship between the loading rate of Hg(II) to the mesocosms and concentrations of spike DGM in surface waters. Bars are the observed values, and diamonds are the expected values assuming concentrations are directly proportional to Hg(II) loading rates.

ability of the Hg(II) substrate in the water column. Our findings are consistent with previous studies that have reported a positive relationship between DGM concentrations and the amount of substrate available in water. For example, when different amounts of Hg(II) were added to water samples from North Lake, Nunavut (Amyot et al., 1997) and Lake 239, ELA (Amyot et al., 2004), concentrations of DGM in the samples after incubation under solar radiation were positively related to the amount of Hg(II) added. Furthermore, DGM concentrations in Arctic lakes are directly proportional to concentrations of dissolved labile mercury in surface waters (Tseng et al., 2004; Tseng, C., personal communication).

3.2. Mass transfer coefficients

Mass transfer coefficients of SF₆ (k_{SF_6}) in the mesocosms ranged from 0.7 to 2.9 cm h⁻¹ during the four sampling periods (Table 2). The highest k_{SF_6} in all three mesocosms were observed during the first sampling period (3–8 July), despite similar wind conditions in all periods. At low wind speeds (below ~2–3 m s⁻¹), such as those experienced in

the mesocosms, gas exchange is not strongly dependent on wind speed, and other processes, such as convective cooling or rain, become more important (Cole and Caraco, 1998; Crusius and Wanninkhof, 2003). k_{SF_6} in Mesocosm 5x tended to be slightly higher than in other mesocosms, but these higher values increased evasion rates by less than 30%, and cannot account for the observed differences in spike DGM concentrations.

To compare the k_{SF_6} observed in the mesocosms with other studies, we normalized our data to a Schmidt number of 600 (Jähne et al., 1987). Normalized mass transfer coefficients (k_{600}) in the mesocosms were in good agreement with previous studies (Table 3). The k_{600} values in the mesocosms were higher than those reported for densely treed, low-wind, experimental reservoirs, and lower than those from exposed English lakes. Most importantly, the k_{600} values in the mesocosms were similar to natural lakes experiencing low to moderate wind conditions. Consequently, we believe the mesocosms are a reasonable model for gas exchange in sheltered lakes.

Based on k_{SF_6} , we calculated mass transfer coefficients for elemental mercury (k_{Hg}) between 1.2 and 4.7 cm h⁻¹

Table 2
Mass transfer coefficients of the tracer sulfur hexafluoride (k_{SF_6}) and elemental mercury (k_{Hg}) across the air–water interface of the mesocosms

Period	Air T ($^{\circ}\text{C}$)	Water T ($^{\circ}\text{C}$)	Wind (m s^{-1})	Rain (mm d^{-1})	k_{SF_6} (cm h^{-1})			k_{Hg} (cm h^{-1})		
					Meso 2 \times	Meso 5 \times	Meso 12 \times	Meso 2 \times	Meso 5 \times	Meso 12 \times
3–8 July	18.7	n/a	1.0	2.5	2.5	2.9	2.5	4.0	4.7	4.0
17–20 July	23.4	26.7	0.8	0.1	1.6	2.0	0.7	2.6	3.2	1.2
31 July–3 August	18.4	23.0	1.0	0.6	1.7	2.4	1.6	2.7	3.8	2.7
14–19 August	15.2	20.0	1.0	4.9	1.5	2.0	1.4	2.4	3.3	2.3

Average daily air and water temperatures, wind speed (1-m height), and rainfall are shown for each period.

Table 3
Comparison of mass transfer coefficients of sulfur hexafluoride from various aquatic ecosystems

Location	k_{600} (cm h^{-1})	Reference
FLUDEX reservoirs, ELA	0.5–0.9	Matthews et al. (2003)
Mesocosm 12 \times	2.0	This study
Mesocosm 2 \times	2.3	This study
Mirror Lake, New Hampshire	2.7	Cole and Caraco (1998)
Lake 658, ELA	2.7	Matthews et al. (2003)
Mesocosm 5 \times	3.0	This study
Crowley Lake, California	3.4	Wanninkhof et al. (1987)
Mono Lake, California	3.4	Wanninkhof et al. (1987)
Sutherland Pond, New York	3.6	Clark et al. (1995)
Lake 302N, ELA	4.0	Crusius and Wanninkhof (2003)
Rockland Lake, New York	4.4	Wanninkhof et al. (1985)
Coatenhill Reservoir, England	4.7	Frost and Upstill-Goddard (2002)
Dozmary Pool, England	6.7	Upstill-Goddard et al. (1990)
Siblyback Lake, England	7.3	Upstill-Goddard et al. (1990)

All mass transfer coefficients were normalized to a Schmidt number of 600 (k_{600}).

(Table 2). This range is in good agreement with k_{Hg} values used for Wisconsin lakes (Fitzgerald et al., 1991; Vandal et al., 1991; Fitzgerald et al., 1994), the Florida Everglades (Lindberg and Zhang, 2000), and Arctic lakes (Amyot et al., 1997; Tseng et al., 2004; Fitzgerald et al., 2005).

3.3. Mercury evasion

Spike DGM evasion rates followed a saw-tooth pattern over time (Fig. 1; bars), corresponding to changes in spike DGM concentrations (Fig. 1; circles). Evasion of spike DGM ranged between 2–7 $\text{ng m}^{-2} \text{h}^{-1}$ in Mesocosm 2 \times , 4–36 $\text{ng m}^{-2} \text{h}^{-1}$ in Mesocosm 5 \times , and 8–36 $\text{ng m}^{-2} \text{h}^{-1}$ in Mesocosm 12 \times . In comparison, evasion rates of ambient DGM for all three mesocosms ranged between 1 and 8 $\text{ng m}^{-2} \text{h}^{-1}$. Note that evasion rates were estimated using DGM concentrations measured between 10:00 and 14:00, and thus represent upper limits. Mercury evasion rates from water bodies in North America are typically around 1–5 $\text{ng m}^{-2} \text{h}^{-1}$ (e.g. Schroeder et al., 1992; O'Driscoll et al., 2003; Hines and Brezonik, 2004), but rates up to

20 $\text{ng m}^{-2} \text{h}^{-1}$ and 50 $\text{ng m}^{-2} \text{h}^{-1}$ have been reported in Sweden (Xiao et al., 1991; Schroeder et al., 1992; Lindberg et al., 1995) and China (Feng et al., 2004), respectively.

Cumulative losses of spike DGM to the atmosphere are shown in Fig. 3 as a percentage of the Hg(II) added to date to each mesocosm. For the first few weeks, the losses in the three mesocosms were similar, but became less so with time. Higher losses in Mesocosm 5 \times were the result of higher-than-expected DGM concentrations on some dates (Fig. 2), and greater k_{Hg} (Table 2). Lower losses in Mesocosm 12 \times were a consequence of reduced k_{Hg} in late July (Table 2). By the end of the 8-week period, we estimate that 38%, 59%, and 33% of the added mercury was lost to the atmosphere from Mesocosms 2 \times , 5 \times , and 12 \times , respectively. Differences in the percentage of mercury lost from each mesocosm were apparently unrelated to the rate of Hg(II) loading (5 \times > 2 \times > 12 \times). In comparison, the cumulative loss of experimentally added mercury from Lake 658, as part of the METAALICUS study, was estimated to be 31–38% over a 20-week period that Hg(II) was added to the whole lake (Southworth, G., personal communication). Losses of this magnitude do not appear to be unique to Hg(II) loading experiments. For example, annual mercury evasion is between 7% and 51% of annual atmospheric mercury deposition in seven Wisconsin lakes (Fitzgerald et al., 1991; Vandal et al., 1991; Watras et al., 1994), and is comparable to, or even exceeds, annual atmospheric mercury deposition in oligotrophic lakes in southwest Sweden (Xiao et al., 1991), and in several Arctic lakes (Tseng et al., 2004; Fitzgerald et al., 2005). Evidently, evasion represents a substantial loss of mercury from many aquatic ecosystems across a broad geographical range.

Together, our data suggest that, under similar environmental conditions, increases in atmospheric mercury deposition to an aquatic ecosystem will result in proportional increases in DGM production and evasion. Our conclusion is constrained to the range in Hg(II) loading rates simulated in our study, and to aquatic ecosystems comparable to our study systems. The findings of this experiment are supported by a previous study where mercury evasion rates in non-manipulated study lakes in Wisconsin generally increased by 2–3 times between 1989 and 1990, coincident with a 3-fold increase in atmospheric deposition of reactive mercury (Fitzgerald et al., 1994). It is not clear, however, whether decreases in atmospheric mercury deposition will result in comparable proportional decreases in DGM pro-

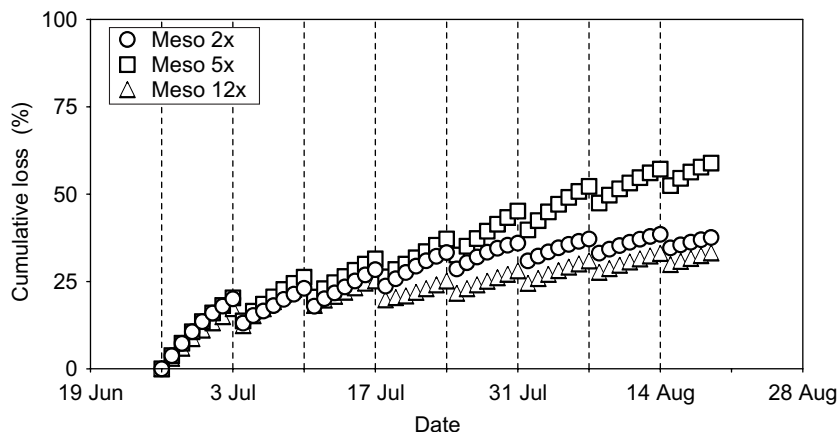


Fig. 3. Cumulative loss of mercury to the atmosphere as a percentage of the Hg(II) added (to date) to each mesocosm. Vertical lines as in Fig. 1.

duction and evasion, since the residence time of newly deposited Hg(II) is not yet confirmed. However, if DGM is only produced from recently deposited mercury, then decreases in atmospheric mercury deposition should result in proportional decreases in DGM production and evasion.

Acknowledgements

This is contribution #19 in the METAALICUS series of publications. We thank John Rudd, Paul Blanchfield, and Reed Harris for input into the experimental design, Danielle Godard, Jane Orihel, and Jason Venkiteswaran for field assistance, Ray Hesslein and Claire Herbert for analyzing SF₆ samples, and the Freshwater Institute for providing water chemistry and meteorological data. We gratefully acknowledge research funding from the Collaborative Mercury Research Network (COMERN) to M.P., M.A., and H.H., and support from the Electric Power Research Institute. We thank Drew Bodaly, Ray Hesslein, Vincent St. Louis, and two anonymous reviewers for their constructive comments on earlier versions of this manuscript.

References

- Alberts, J.J., Schindler, J.E., Miller, R.W., Nutter Jr., D.E., 1974. Elemental mercury evolution mediated by humic acid. *Science* 184, 895–897.
- Amyot, M., Lean, D., Mierle, G., 1997. Photochemical formation of volatile mercury in high Arctic lakes. *Environ. Toxicol. Chem.* 16, 2054–2063.
- Amyot, M., Lean, D.R.S., Poissant, L., Doyon, M.-R., 2000. Distribution and transformation of elemental mercury in the St. Lawrence River and Lake Ontario. *Can. J. Fish. Aquat. Sci.* 57 (S1), 155–163.
- Amyot, M., Mierle, G., Lean, D.R.S., McQueen, D.J., 1994. Sunlight-induced formation of dissolved gaseous mercury in lake waters. *Environ. Sci. Technol.* 28, 2366–2371.
- Amyot, M., Southworth, G., Lindberg, S.E., Hintelmann, H., Lalonde, J.D., Ogrinc, N., Poulain, A.J., Sandilands, K.A., 2004. Formation and evasion of dissolved gaseous mercury in large enclosures amended with ²⁰⁰HgCl₂. *Atmos. Environ.* 38, 4279–4289.
- Boucher, D.F., Alves, G.E., 1959. Dimensionless numbers. *Chem. Eng. Prog.* 55, 55–64.
- Clark, J.F., Schlosser, P., Wanninkhof, R., Simpson, H.J., Schuster, W.S.F., Ho, D.T., 1995. Gas transfer velocities for SF₆ and ³He in a small pond at low wind speeds. *Geophys. Res. Lett.* 22, 93–96.
- Cole, J.J., Caraco, N.F., 1998. Atmospheric exchange of carbon dioxide in a low-wind oligotrophic lake measured by the addition of SF₆. *Limnol. Oceanogr.* 43, 647–656.
- Crusius, J., Wanninkhof, R., 2003. Gas transfer velocities measured at low wind speed over a lake. *Limnol. Oceanogr.* 48, 1010–1017.
- Feng, X., Yan, H., Wang, S., Qiu, G., Tang, S., Shang, L., Dai, Q., Hou, Y., 2004. Seasonal variation of gaseous mercury exchange rate between air and water surface over Baihua reservoir, Guizhou, China. *Atmos. Environ.* 38, 4721–4732.
- Fitzgerald, W.F., Engstrom, D.R., Lamborg, C.H., Tseng, C.-M., Balcom, P.H., Hammerschmidt, C.R., 2005. Modern and historic atmospheric mercury fluxes in northern Alaska: global sources and Arctic depletion. *Environ. Sci. Technol.* 39, 557–568.
- Fitzgerald, W.F., Engstrom, D.R., Mason, R.P., Nater, E.A., 1998. The case for atmospheric mercury contamination in remote areas. *Environ. Sci. Technol.* 32, 1–7.
- Fitzgerald, W.F., Mason, R.P., Vandal, G.M., 1991. Atmospheric cycling and air–water exchange of mercury over mid-continental lacustrine regions. *Water, Air, Soil Pollut.* 56, 745–767.
- Fitzgerald, W.F., Mason, R.P., Vandal, G.M., Dulac, F., 1994. Air–water cycling of mercury in lakes. In: Watras, C.J., Huckabee, J.W. (Eds.), *Mercury Pollution: Integration and Synthesis*. Lewis Publishers, Boca Raton, United States, pp. 203–220.
- Frost, T., Upstill-Goddard, R.C., 2002. Meteorological controls of gas exchange at a small English lake. *Limnol. Oceanogr.* 47, 1165–1174.
- Ganguli, P.M., Mason, R.P., Abu-Saba, K.E., Anderson, R.S., Flegal, A.R., 2000. Mercury speciation in drainage from the New Idria mercury mine, California. *Environ. Sci. Technol.* 34, 4773–4779.
- Hines, N.A., Brezonik, P.L., 2004. Mercury dynamics in a small Northern Minnesota lake: water to air exchange and photoreactions of mercury. *Mar. Chem.* 90, 137–149.
- Hintelmann, H., Ogrinc, N., 2003. Determination of stable mercury isotopes by ICP/MS and their application in environmental studies. *ACS Symp. Ser.* 835, 321–338.
- Jackson, T.A., 1997. Long-range atmospheric transport of mercury to ecosystems, and the importance of anthropogenic emissions – a critical review and evaluation of the published evidence. *Environ. Rev.* 5, 99–120.
- Jähne, B., Münnich, K.O., Bösinger, R., Dutzi, A., Huber, W., Libner, P., 1987. On the parameters influencing air–water gas exchange. *J. Geophys. Res.* 92, 1937–1949.
- Lindberg, S.E., Meyers, T.P., Munthe, J., 1995. Evasion of mercury vapor from the surface of a recently limed acid forest lake in Sweden. *Water, Air, Soil Pollut.* 85, 725–730.

- Lindberg, S.E., Vette, A.F., Miles, C., Schaedlich, F., 2000. Mercury speciation in natural waters: measurement of dissolved gaseous mercury with a field analyzer. *Biogeochemistry* 48, 237–259.
- Lindberg, S.E., Zhang, H., 2000. Air/water exchange of mercury in the Everglades II: measuring and modeling evasion of mercury from surface waters in the Everglades Nutrient Removal Project. *Sci. Total Environ.* 259, 135–143.
- Liss, P.S., Slater, P.G., 1974. Flux of gases across the air–sea interface. *Nature* 247, 181–184.
- Mason, R.P., Morel, F.M.M., Hemond, H.F., 1995. The role of microorganisms in elemental mercury formation in natural waters. *Water, Air, Soil Pollut.* 80, 775–787.
- Matthews, C.J.D., St. Louis, V.L., Hesslein, R.H., 2003. Comparison of three techniques used to measure diffusive gas exchange from sheltered aquatic surfaces. *Environ. Sci. Technol.* 37, 772–780.
- O'Driscoll, N.J., Beauchamp, S., Siciliano, S.D., Rencz, A.N., Lean, D.R.S., 2003. Continuous analysis of dissolved gaseous mercury (DGM) and mercury flux in two freshwater lakes in Kejimikujik Park, Nova Scotia: evaluating mercury flux models with quantitative data. *Environ. Sci. Technol.* 37, 2226–2235.
- Orihel, D.M., 2005. The effects of changes in atmospheric deposition on the bioaccumulation of mercury by fish. M.N.R.M. Thesis. Natural Resources Institute, University Of Manitoba, Winnipeg, Canada, p. 190.
- Poissant, L., Amyot, M., Pilote, M., Lean, D., 2000. Mercury water–air exchange over the Upper St. Lawrence River and Lake Ontario. *Environ. Sci. Technol.* 34, 3069–3078.
- Poulain, A.J., Amyot, M., Findlay, D., Telor, S., Barkay, T., Hintelmann, H., 2004. Biological and photochemical production of dissolved gaseous mercury in a boreal lake. *Limnol. Oceanogr.* 49, 2265–2275.
- Sanemasa, I., 1975. The solubility of elemental mercury vapor in water. *Bull. Chem. Soc. Jpn.* 48, 1795–1798.
- Schroeder, W., Lindqvist, O., Munthe, J., Xiao, Z., 1992. Volatilization of mercury from lake surfaces. *Sci. Total Environ.* 125, 47–66.
- Siciliano, S.D., O'Driscoll, N.J., Lean, D.R.S., 2002. Microbial reduction and oxidation of mercury in freshwater lakes. *Environ. Sci. Technol.* 36, 3064–3068.
- St. Louis, V.L., Rudd, J.W.M., Kelly, C.A., Hall, B.D., Rolffus, K.R., Scott, K.J., Lindberg, S.E., Dong, W., 2001. Importance of the forest canopy to fluxes of methyl mercury and total mercury to boreal ecosystems. *Environ. Sci. Technol.* 35, 3089–3098.
- Tseng, C.M., Lamborg, C., Fitzgerald, W.F., Engstrom, D.R., 2004. Cycling of dissolved elemental mercury in Arctic Alaskan lakes. *Geochim. Cosmochim. Acta* 68, 1173–1184.
- Upstill-Goddard, R.C., Watson, A.J., Liss, P.S., Liddicoat, M.I., 1990. Gas transfer velocities in lakes measured with SF₆. *Tellus* 42B, 364–377.
- Vandal, G.M., Fitzgerald, W.F., Rolffus, K.R., Lamborg, C.H., 1995. Modeling the elemental mercury cycle in Pallette Lake, Wisconsin, USA. *Water, Air, Soil Pollut.* 80, 529–538.
- Vandal, G.M., Mason, R.P., Fitzgerald, W.F., 1991. Cycling of volatile mercury in temperate lakes. *Water, Air, Soil Pollut.* 56, 791–803.
- Wanninkhof, R., 1992. Relationship between wind speed and gas exchange over the ocean. *J. Geophys. Res.* 97, 7373–7382.
- Wanninkhof, R., Ledwell, J.R., Broecker, W.S., 1985. Gas exchange–wind speed relation measured with sulfur hexafluoride on a lake. *Science* 227, 1224–1226.
- Wanninkhof, R., Ledwell, J.R., Broecker, W.S., Hamilton, M., 1987. Gas exchange on Mono Lake and Crowley Lake, California. *J. Geophys. Res.* 92, 14567–14580.
- Watras, C.J., Bloom, N.S., Hudson, R.J.M., Gherini, S., Munson, R., Claas, S.A., Morrison, K.A., Hurley, J., Wiener, J.G., Fitzgerald, W.F., Mason, R., Vandal, G., Powell, D., Rada, R., Rislov, L., Winfrey, M., Elder, J., Krabbenhoft, D., Andren, A.W., Babiarz, C., Porcella, D.B., Huckabee, J.W., 1994. Sources and fates of mercury and methylmercury in Wisconsin Lakes. In: Watras, C.J., Huckabee, J.W. (Eds.), *Mercury Pollution: Integration and Synthesis*. Lewis Publishers, Boca Raton, United States, pp. 153–177.
- Xiao, Z.F., Munthe, J., Schroeder, W.H., Lindqvist, O., 1991. Vertical fluxes of volatile mercury over forest soil and lake surfaces in Sweden. *Tellus* 43B, 267–279.